Journal of Magnetic Resonance **145,** 147–151 (2000)
doi:10.1006/jmre.2000.2103, available online at http://www.idealibrary.com on IDEAL®

Sensitivity-Enhanced MQ–HCN–CCH–TOCSY and MQ–HCN–CCH–COSY Pulse Schemes for $^{13}C/^{15}N$ Labeled RNA Oligonucleotides

Weidong Hu,[1] Licong Jiang, and Yuying Q. Gosser

Memorial Sloan-Kettering Cancer Center, Box 557, 1275 York Avenue, New York, New York 10021

Received December 20, 1999; revised April 6, 2000

Sensitivity enhanced multiple-quantum 3D HCN–CCH–TOCSY and HCN–CCH–COSY experiments are presented for the ribose resonance assignment of $^{13}C/^{15}N$-labeled RNA sample. The experiments make use of the chemical shift dispersion of N1/N9 of pyrimidine/purine to distinguish the ribose spin systems. They provide a complementary approach for the assignment of ribose resonance to the currently used HCCH–COSY and HCCH–TOCSY type experiments in which either ^{13}C or ^{1}H is utilized to separate the different ribose spin systems. The pulse schemes have been demonstrated on a 23-mer $^{13}C/^{15}N$-labeled RNA aptamer complexed with neomycin and tested on a 32-mer RNA complexed with a 23-residue peptide.

Key Words: **sensitivity enhancement; multiple-quantum coherence; HCN–CCH–TOCSY; HCN–CCH–COSY; assignment; RNA.**

The HCCH–COSY (*1–3*) and HCCH–TOCSY (*3–5*) type experiments are most widely used for the ribose resonance assignment for ^{13}C-labeled RNA. The poor chemical shift dispersion of both ^{1}H and ^{13}C in ribose makes the assignment a difficult task for a larger-sized RNA. To overcome this problem, extension and modification of the above two kinds of experiments have been presented such as the HCCH–RELAY (*3*), the high-resolution constant-time 2D or 3D HCCH–COSY/TOCSY (*6*), and the HCCH–COSY–TOCSY experiment (*7*). On the other hand, the ribose assignment of a larger-sized RNA can also be tackled by selectively labeling different nucleotides (*6, 8*). Recently, single and multiple quantum HCN–CCH–TOCSY experiments (*9, 10*) have been reported in which the N1/N9 of pyrimidine/purine are used to separate the ribose spin systems instead of relying on the poorly resolved proton and carbon. In this study, we propose sensitivity-enhanced MQ–HCN–CCH–TOCSY and a novel se-MQ–HCN–CCH–COSY experiments as a complementary approach for the ribose resonance assignment.

[1] To whom correspondence should be addressed. Fax: (212) 717-3453; E-mail: weidong@sbnmr1.ski.mskcc.org.

The magnetization transfer schemes for the HCN–CCH–TOCSY and HCN–CCH–COSY are

$$H1' \rightarrow C1' \rightarrow N1/N9(t1) \rightarrow C1' \rightarrow Cn'(t2) \rightarrow Hn'(t3)$$

and

$$H1' \rightarrow C1' \rightarrow N1/N9(t1) \rightarrow C1' \rightarrow C1'/C2'(t2) \rightarrow H1'/H2'(t3),$$

respectively, where the $n = 1, 2, 3, 4, 5$ stands for the carbons and protons in the ribose ring. Compared to the chemical shift dispersions of carbon and proton in ribose, the chemical shifts of N1/N9 of pyrimidine/purine are well separated, and the dispersion within each group (U, C, G, and A) is reasonably good, about 4 ppm for U, 6 ppm for C, and 6 ppm for G and A (*11*). Thus the resonance of ^{1}H and ^{13}C in the ribose spin system might be distinguishable by the nitrogen dimension in the HCN–CCH–TOCSY experiment if they are not in the HCCH–TOCSY experiment. The HCN–CCH–COSY experiment can be used to distinguish the C2′/H2′ from C3′/H3′ whenever an ambiguity exists. In order to make the proposed HCN-type experiments useful to larger-sized RNA samples, the sensitivity optimization is very critical because the J couplings between C1′ and N1/N9 are about 11 Hz (*11*). By taking advantage of the favorable relaxation rate of multiple-quantum coherence (*12*) and following the pioneer application of this phenomenon to nucleic acids (*13–15*), a multiple-quantum version of HCN–CCH–TOCSY was proposed recently (*10*), which enhanced the sensitivity by a factor of 2 over the corresponding single quantum HCN–CCH–TOCSY. Here we present a more sensitive HCN–CCH–TOCSY and a novel se-MQ–HCN–CCH–COSY scheme for larger-sized nucleic acids or the sample with limited concentration.

1090-7807/00 $35.00

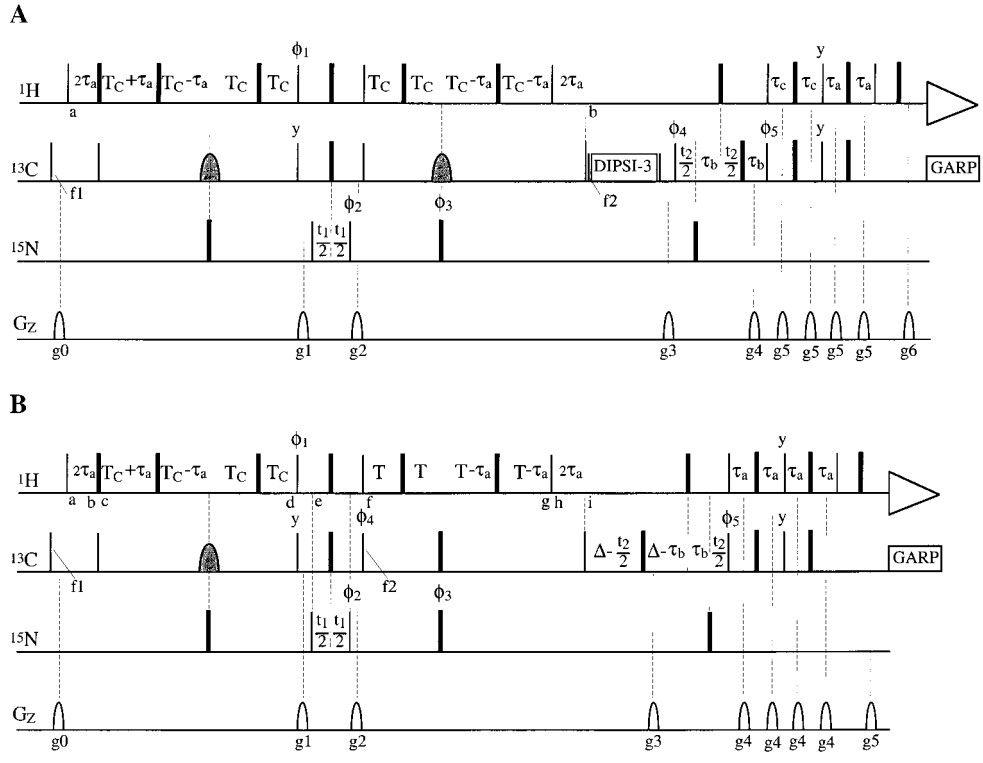

FIG. 1. Pulse schemes of the 3D se-MQ–HCN–CCH–TOCSY (A) and se-MQ–HCN–CCH–COSY (B) for ^{13}C, ^{15}N-labeled RNA. Narrow and wide bars represent 90° and 180° pulses, respectively. All pulses are along the *x*-axis unless otherwise indicated. The shaped pulses on carbon are 180° on-resonance band-selective reburp pulses (*22*) centered at 91 ppm with duration of 2.4 ms for 1A, and 2.7 ms for 1B. The ^{1}H and ^{15}N carrier frequencies were 4.75 and 158 ppm, respectively. The ^{13}C carrier frequency was initially put at 91 ppm at point f1 in 1A and 1B, and then moved to 79 ppm for 1A and 86 ppm for 1B at point f2. Field strengths of the ^{1}H pulse, ^{13}C high power pulse, DIPSI-3 mixing (*23*), GARP decoupling (*24*) on ^{13}C, and ^{15}N pulse were 30.7, 20, 8.6, 2.5, and 7.5 kHz, respectively. Field strengths of carbon reburp pulse for 1A and 1B were 205 and 185 Hz, respectively. Strengths and duration of gradients for 1A were $g0$ = (9 G/cm, 0.2 ms), $g1$ = (−28 G/cm, 0.5 ms), $g2$ = (24 G/cm, 0.5 ms), $g3$ = (−28 G/cm, 0.5 ms), $g4$ = (34 G/cm, 0.8 ms), $g5$ = (9 G/cm, 0.2 ms), $g6$ = (34 G/cm, 0.2 ms). Strengths and duration of gradients for 1B were $g0$ = (9 G/cm, 0.2 ms), $g1$ = (−28 G/cm, 0.5 ms), $g2$ = (24 G/cm, 0.5 ms), $g3$ = (34 G/cm, 0.8 ms), $g4$ = (9 G/cm, 0.2 ms), $g5$ = (34 G/cm, 0.2 ms). ^{13}C-TOCSY mixing time was 18.9 ms. τ_a = 1.5 ms, τ_b = 0.95 ms, 1.5 ms for 1A and 1B, respectively, τ_c = 0.78 ms, T_C = 9 ms, and T = 7.5 ms. Phase cycling was $\phi_1 = y, -y$; $\phi_2 = 4(x), 4(-x)$; $\phi_3 = x$; $\phi_4 = y, y, -y, -y$; $\phi_5 = x$ and Acq. = $x, -x, -x, x, -x, x, x, -x$. Quadrature detection for t_1 was achieved via States–TPPI (*25*) on ϕ_2 and ϕ_3 for both 1A and 1B. For each t_2 increment, the axial peaks were moved to the edges of the spectra by inversion of ϕ_4 and the receiver phase simultaneously for both 1A and 1B (*25*). The *P*- and *N*-type coherence selections for t_2 were achieved by inversion of gradient of G6 for 1A and G5 for 1B in concert with inversion of ϕ_5. The absorption mode for t_2 was achieved by shuffling the raw data as described in (*16*, *17*).

The proposed sequences se-MQ–HCN–CCH–TOCSY and se-MQ–HCN–CCH–COSY are shown in Figs. 1A and 1B, respectively. The coherence transfer pathway from point a to b in Fig. 1A has been described before (*10*). The difference between the current scheme and the previous one is that there are two reverse INEPT units after the carbon chemical shift evolution, which are used to recover both *x* and *y* components of carbons to enhance the sensitivity (*16*). The gradients G3 and G6 are used for coherence selection (*17*). The delay τ_c for the first INEPT is $1/(8 \times J_{C-H})$ so that the sensitivity of both CH and CH_2 moieties can be enhanced, theoretically, by a factor of 1.7 and 1.4, respectively (*18*). The coherence transfer pathway from point a to i in Fig. 1B can be described schematically using product operators (*19*):

$$H1_Z \xrightarrow{a} -H1_Y \xrightarrow{b} H1_XC1_Z \xrightarrow{c}$$

$$-H1_XC1_Y \xrightarrow{d} H1_XC1_XN_Z \xrightarrow{e}$$

$$-H1_ZC1_ZN_Y \xrightarrow{f} H1_YC1_XN_Z \xrightarrow{g} H1_YC1_Y$$

$$-H1_YC1_XC2_Z \xrightarrow{h} H1_ZC1_Y - H1_ZC1_XC2_Z \xrightarrow{i}$$

$$-C1_X + C1_ZC2_Y.$$

The H1, C1, and C2 are the H1′, C1′, and C2′ of the ribose, and N stands for the N1 of pyrimidine or N9 of purine. During 2Δ constant period, both chemical shifts of C1′ and C2′ are evolved, and the antiphase term $C1_ZC2_Y$ is refocused. The two reverse INEPT periods following the 2Δ period are used to enhance the sensitivity (*16*). The coherence selection is achieved by the two gradients G3 and G5 (*17*). The advantage of using reburp pulse on C1′ in the 4 × Tc periods has been discussed before (*10, 15*). In the 4 × T period ($\sim 5/(4 \times J_{C-C})$) in 1B, the hard 180 pulse is used for carbon so that the evolution of C1′ antiphase with respect to C2′ and the refocusing of C1′ antiphase with respect to N1/N9 are concatenated in the same period. During the long transfer step from C1′ to N1/N9 and back in sequence 1A, the transverse magnetization of C1′ exists as a mixture of two-spin and three-spin heteronuclear multiple-quantum coherence with the three-spin coherence antiphase with respect to N1/N9. During the 4 × Tc period in sequence 1B, the C1′ magnetization is in the same situation as in the sequence 1A. While in the 4 × T period, the C1′ magnetization is composed of two-, three-, and four-spin heteronuclear multiple-quantum coherence. The three-spin coherence includes the antiphase with respect to N1/N9 or C2′, and the four-spin coherence is antiphase with respect to both C2′ and N1/N9. Since the T_1 values of N1/N9 and C2′ are usually much larger than the time scale of 4 × T (30 ms in this study), the favorable relaxation rate of multiple-quantum coherence is thus not diminished much by the existence of these three- and four-spin terms, especially when a molecule is large. In short, slow relaxation of multiple quantum coherence during the long magnetization transfer steps between C1′ and N1/N9 can be used to enhance the signal intensity as evidenced in the earlier studies (*10, 13–15*).

The pulse sequences of se-MQ–HCN–CCH–TOCSY and se-MQ–HCN–CCH–COSY were tested on two RNA samples dissolved in D_2O. The one is a 1.8 mM uniformly ^{13}C, ^{15}N-labeled 23-mer RNA aptamer complexed with neomycin B, and the other is a 1.5 mM uniformly ^{13}C, ^{15}N-labeled 32-mer RNA aptamer complexed with a 23-residue. The sequence of the 23-mer aptamer is GGACUGGGCGAGAAGUUUA-GUCC numbered as G_4 to C_{26} (*20*). The 32-mer RNA and peptide complex is an on-going project. All the experiments were carried out on a Varian Inova 500-MHz spectrometer equipped with actively shielded performa II Z-gradients at 25°C. The data was processed and analyzed using FELIX 97.0 (Molecular Simulations) and nmrPipe (*21*) software on an SGI O2 workstation.

The sensitivity enhancement with gradient coherence selection is a well-established method for reasonable-sized biomolecules (*16, 17*). As the size of biomolecules increases, the gained sensitivity for the CH_n group (where *n* can be 1 to 3) is compromised by the signal loss due to the more T_2 relaxation from the extra INEPT step. To find out the applicable range of the se-MQ–HCN–CCH–TOCSY scheme, we collected the data on two RNA samples with different sizes as mentioned above using the MQ–HCN–CCH–TOCSY sequence with and without the sensitivity-enhanced technique under the same experimental conditions. Figures 2A to 2D are the 1D slices from 3D data acquired on the 23-mer RNA aptamer. The H5′/H5″ 1D slices of C26 base with ^{15}N at 152.5 ppm and ^{13}C at 65.5 ppm are shown in Fig. 2A from MQ–HCN–CCH–TOCSY and Fig. 2B from se-MQ–HCN–CCH–TOCSY. The enhancement factor for this CH_2 group is, from the average of the two peaks, 1.4. Figures 2C and 2D are the H1′ 1D slices of C26 with ^{15}N at 152.5 ppm and ^{13}C at 93.1 ppm obtained using MQ–HCN–CCH–TOCSY and se-MQ–HCN–CCH–TOCSY sequences, respectively. The enhancement for this

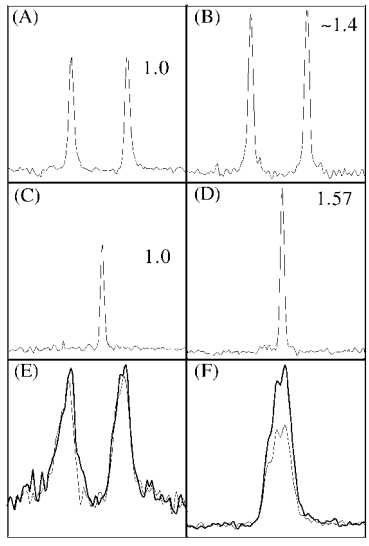

FIG. 2. Comparison of signal intensity of 1D slices from 3D data (A to D) acquired on 23-mer RNA aptamer and 2D data (E and F) acquired on 32-mer RNA complexed with 23-residue peptide using MQ–HCN–CCH–TOCSY with and without sensitivity enhancement scheme. (A) and (C) are the 1D-proton slices of C26 base from 3D spectra acquired using the MQ–HCN–CCH–TOCSY, and (B) and (D) are from se-MQ–HCN–CCH–TOCSY sequence. The spectral width (Hz)/complex points along ^{15}N, ^{13}C, and ^{1}H dimensions were 1621/36, 4274/34, and 6000/512 with 32 transients per FID for both experiments. The total experimental time is 52.5 h. All other related parameters are the same as in the legend to Fig. 1A. The ^{15}N dimension resolution was enhanced through linear prediction (*21*) resulting in a final matrix size of 128 × 128 × 512. The (A) and (B) are the 1D proton slices of H5′/H5″ with ^{15}N and ^{13}C at 152.5 and 65.5 ppm obtained using MQ–HCN–CCH–TOCSY and se-MQ–HCN–CCH–TOCSY sequences, respectively. They are scaled to the same noise level. The average intensity of two H5 peaks in (B) is about 1.4-fold larger than that in (A). The (C) and (D) are the 1D proton slices of H1′ with ^{15}N and ^{13}C at 152.5 and 93.1 ppm obtained from MQ–HCN–CCH–TOCSY and se-MQ–HCN–CCH–TOCSY sequences, respectively. They are scaled to the same noise level. The intensity of H1′ peak in (D) is about 1.57-fold larger than that in (C). For (E) and (F), the spectral width (Hz)/complex points along ^{13}C and ^{1}H dimensions were 4274/34 and 6000/512 with 320 transients per FID for both experiments. The thick lines in both (E) and (F) are from se-MQ–HCN–CCH–TOCSY, and the thin lines are from MQ–HCN–CCH–TOCSY sequence. (E) shows the signal from CH_2 group with ^{13}C positioned at 64.1 ppm; the intensity of the thick line is about 5% larger than that of thin line. (F) shows the signal from CH group with ^{13}C at 81.8 ppm, the intensity of the thick line is about 45% larger than that of thin line.

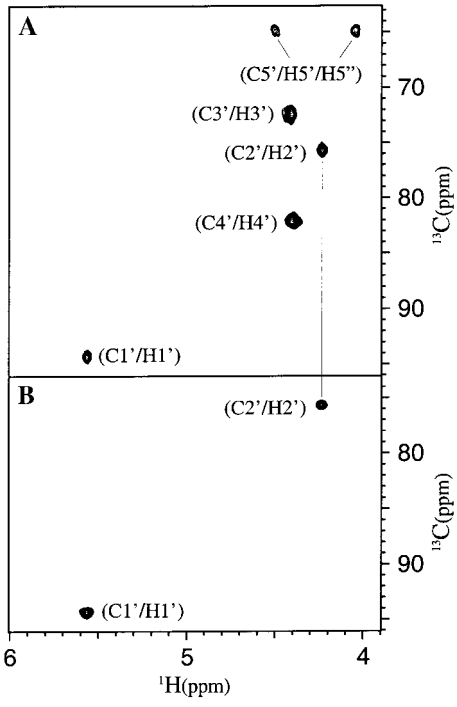

FIG. 3. 2D planes of base C25 with ^{15}N at 152 ppm acquired using 3D se-MQ–HCN–CCH–TOCSY (A) and se-HCN–CCH–COSY (B) on the uniformly ^{13}C/^{15}N labeled 23 mer RNA aptamer complexed with neomycin. The experimental parameters for (A) have been given in the figure legend to Fig. 2. The spectral widths (Hz)/complex points along ^{15}N, ^{13}C, and ^{1}H were 1621/36, 3016/20, and 6000/512, respectively, with 24 transients per FID for (B). The total experimental time is 23 h. The ^{15}N dimension resolution was enhanced through linear prediction (*21*) resulting in a final matrix size of 128 × 128 × 512. The C2′/H2′ resonance of the ribose C25 was easily assigned from the se-HCN–CCH–COSY experiment (B). Thus, the C2′/H2′ resonance in plane (A) was identified (connected by the thin line to the C2′/H2′ in (B)), and the complete resonance for ribose of C25 was thus assigned and labeled in (A).

CH group is 1.57. Out of four evaluated bases, the enhancement factors for CH5′/5″ and CH1′ are, on average, 1.22 and 1.66, respectively. Figures 2E and 2F are from 2D ^{1}H–^{13}C plane acquired on a 32-mer RNA complexed with a 23-residue peptide. The thick and thin lines are from se-MQ–HCN–CCH–TOCSY and MQ–HCN–CCH–TOCSY sequences, respectively, under the same experimental conditions. Figure 2E shows the signal of CH_2 groups with ^{13}C anchored at 64.1 ppm, where 2F shows the profile of CH groups with ^{13}C positioned at 81.8 ppm. The enhancement for CH_2 and CH are about 5 and 45%, respectively. Since the 32-mer RNA and 23-residue complex is equivalent to a 39-mer RNA in molecular weight, the result suggests that the CH group signal can be enhanced significantly for large-sized RNA samples in the se-MQ–HCN–CCH–TOCSY experiment, where the enhancement for the CH_2 group for large-sized samples is marginal and well below the theoretical prediction (*18*).

In the original structural study of the 23-mer RNA aptamer (*20*), a near complete resonance assignment for the ribose has been achieved using the combination of HCCH–COSY–TOCSY and ^{13}C-edited NOESY experiments except for the bases U8 and C25. Their H1′ chemical shifts are almost superimposed with five other H1′ protons, and the dispersion of their C1′ chemical shifts is also poor (*20*). But the problem can be solved if N1/N9 is used to separate the ribose spin systems in the MQ–HCN–CCH experiment (*10*). Here the application of se-MQ–HCN–CCH–TOCSY and se-MQ–HCN–CCH–COSY is demonstrated in Figs. 3A and 3B for base C25. Both 3A and 3B are 2D planes anchored at 151.6 ppm along ^{15}N dimension. Since there are no other bases whose N1 (N9 is located in a much lower field (*11*)) is nearby on the scale of resolution along ^{15}N dimension (*10*), the resonance of this spin system can be easily assigned by the combination of the two experiments and labeled in the figure. Thus the combination of these two experiments can be used as a complementary approach when ribose spin systems cannot be resolved using HCCH–COSY, HCCH–TOCSY, and HCCH–COSY–TOCSY experiments.

In summary, sensitivity-enhanced se-MQ–HCN–CCH–TOCSY and se-MQ–HCN–CCH–COSY experiments for ribose assignment are presented. The experiments, using N1/N9 to distinguish the ribose spin systems, are useful complementary methods to the HCCH–COSY and HCCH–TOCSY type experiments in which the separation of ribose spin systems relies on poorly dispersed protons or carbons. The sensitivity of the CH group can be increased significantly by using Rance–Kay sensitivity enhancement scheme on both medium- and large-sized RNA complexes, while the enhancement for the CH_2 group of a large-sized RNA sample is marginal. Combined with se-MQ–HCN–CCH–COSY, the more sensitive HCN–CCH–TOCSY experiment provides an applicable complementary method for HCCH–COSY and HCCH–TOCSY in the ribose resonance assignment of RNA samples up to 40 nucleotides.

ACKNOWLEDGMENTS

We thank Dr. D. J. Patel for encouragement and helpful discussions during the course of the work. This research was funded by NIH Grant GM-54777 to Dr. D. J. Patel.

REFERENCES

1. A. Bax, G. M. Clore, P. C. Driscoll, A. M. Gronenborn, M. Ikura, and L. E. Kay, Practical aspects of proton–carbon–carbon–proton three-dimensional correlation spectroscopy of ^{13}C-labeled proteins, *J. Magn. Reson.* **87,** 620–627 (1990).
2. L. E. Kay, M. Ikura, and A. Bax, Proton–proton correlation via carbon–carbon couplings: A three-dimensional NMR approach for the assignment of aliphatic resonances in proteins labeled with carbon-13, *J. Am. Chem. Soc.* **112,** 888–889 (1990).
3. E. P. Nikonowicz and A. Pardi, An efficient procedure for assignment of the proton, carbon and nitrogen resonances in ^{13}C/^{15}N labeled nucleic acids, *J. Mol. Biol.* **232,** 1141–1156 (1993).

4. S. W. Fesik, H. L. Eaton, E. T. Olejniczak, and E. R. P. Zuiderweg, 2D and 3D NMR-spectroscopy employing ^{13}C–^{13}C magnetization transfer by isotropic mixing. Spin system identification in large proteins, *J. Am. Chem. Soc.* **112,** 886–888 (1990).
5. A. Bax, G. M. Clore, and A. M. Gronenborn, ^{1}H–^{1}H correlation via isotropic mixing of ^{13}C magnetization, a new three-dimensional approach for assigning ^{1}H and ^{13}C spectra of ^{13}C-enriched proteins, *J. Magn. Reson.* **88,** 425–431 (1990).
6. M. H. Kolk, S. S. Wijmenga, H. A. Heus, and C. W. Hilbers, On the NMR structure determination of a 44n RNA pseudoknot: Assignment strategies and derivation of torsion angle restraints, *J. Biomol. NMR* **12,** 423–433 (1998).
7. W. Hu, L. T. Kakalis, L. Jiang, F. Jiang, X. Ye, and A. Majumdar, 3D HCCH–COSY–TOCSY experiment for the assignment of ribose and amino acid side chains in ^{13}C labeled RNA and protein, *J. Biomol. NMR* **12,** 559–564 (1998).
8. M. H. Kolk, M. van der Graaf, S. S. Wijmenga, C. W. A. Pleij, H. A. Heus, and C. W. Hilbers, NMR structure of a classical pseudoknot: Interplay of single- and double-stranded RNA, *Science* **280,** 434–438 (1998).
9. R. Ramachandran, C. Sich, M. Grune, V. Soskic, and L. R. Brown, Sequential assignments in uniformly ^{13}C- and ^{15}N-labeled RNAs: The HC(N,P) and HC(N,P)–CCH–TOCSY experiments, *J. Biomol. NMR* **7,** 251–255 (1996).
10. W. Hu and L. Jiang, Multiple-quantum HCN–CCH–TOCSY experiment for $^{13}C/^{15}N$ labeled RNA oligonucleotides, *J. Biomol. NMR* **15,** 289–293 (1999).
11. S. S. Wijmenga and B. N. M. van Buuren, The use of NMR methods for conformational studies of nucleic acids, *Prog. Nuclear Magn. Res. Spectrosc.* **32,** 287–387 (1998).
12. S. Grzesiek and A. Bax, Spin-locked multiple quantum coherence for signal enhancement in heteronuclear multidimensional NMR experiments, *J. Biomol. NMR* **6,** 335–339 (1995).
13. J. P. Marino, J. L. Diener, P. B. Moore, and C. Griesinger, Multiple-quantum coherence dramatically enhances the sensitivity of CH and CH_2 correlation in uniformly ^{13}C-labeled RNA, *J. Am. Chem. Soc.* **119,** 7361–7366 (1997).
14. V. Sklenár, T. Dieckmann, S. E. Butcher, and J. Feigon, Optimization of triple-resonance HCN experiments for application to larger RNA oligonucleotides, *J. Magn. Reson.* **130,** 119–124 (1998).
15. R. Fiala, F. Jiang, and V. Sklenár, Sensitivity optimized HCN and HCNCH experiments for $^{13}C/^{15}N$ labeled oligonucleotides, *J. Biomol. NMR* **12,** 373–383 (1998).
16. J. Cavanagh and M. Rance, Sensitivity-enhanced NMR techniques for the study of biomolecules, *Annu. Rep. NMR Spectrosc.* **27,** 1–58 (1993).
17. L. E. Kay, P. Keifer, and T. Saarinen, Pure absorption gradient enhanced heteronuclear single quantum correlation spectroscopy with improved sensitivity, *J. Am. Chem. Soc.* **114,** 10663–10665 (1992).
18. J. Schleucher, M. Schwendinger, M. Sattler, P. Schmidt, O. Schedletzky, S. J. Glaser, O. W. Sorensen, and C. Griesinger, A general enhancement scheme in heteronuclear multidimensional NMR employing pulsed field gradients, *J. Bimol. NMR* **4,** 301–306 (1994).
19. O. W. Sørensen, G. W. Eich, M. H. Levitt, G. Bodenhausen, and R. R. Ernst, Product operator formalism for the description of NMR pulse experiments, *Prog. NMR Spectrosc.* **16,** 163–192 (1983).
20. L. Jiang, A. Majumdar, W. Hu, T. J. Jaishree, W. Xu, and D. J. Patel, Saccharide–RNA recognition in a complex formed between neomycin B and an RNA Aptamer, *Structure Fold Des.* **7,** 817–827 (1999).
21. F. Delaglio, S. Grzesiek, G. Vuister, G. Zhu, J. Pfeiffer, and A. Bax, NMRPipe: A multidimensional spectral processing system based on UNIX pipes, *J. Biomol. NMR* **6,** 277–293 (1995).
22. H. Geen and R. Freeman, Band-selective radio frequency pulses, *J. Magn. Res.* **93,** 93–141 (1991).
23. A. J. Shaka, C. J. Lee, and A. Pines, Iterative schemes for bilinear operations: Application to spin decoupling, *J. Magn. Reson.* **77,** 274–293 (1988).
24. A. J. Shaka, P. B. Barker, and R. Freeman, Computer-optimized decoupling scheme for wide band applications and low-level operation, *J. Magn. Reson.* **64,** 547–552 (1985).
25. D. Marion, M. Ikura, R. Tschudin, and A. Bax, Rapid recording of 2D NMR spectra without phase cycling. Application to the study of hydrogen exchange in proteins, *J. Magn. Reson.* **85,** 393–399 (1989).